A novel strong green phosphor: $K_3Gd(PO_4)_2$:Ce^{3+}, Tb^{3+} for a UV-excited white light-emitting-diode*

Jiang Ting-Ming(姜庭明)[a], Yu Xue(余 雪)[a)b)], Xu Xu-Hui(徐旭辉)[a)b)], Zhou Da-Cheng(周大成)[a)b)], Yu Hong-Ling(余红玲)[a)], Yang Peng-Hui(杨鹏辉)[a)], and Qiu Jian-Bei(邱建备)[a)b)†]

[a)] *College of Materials Science and Engineering, Kunming University of Science and Technology, Kunming* 650093, *China*
[b)] *Key Laboratory of Advanced Materials of Yunnan Province, Kunming* 650093, *China*

(Received 20 May 2013; revised manuscript received 14 June 2013; published online 20 December 2013)

A series of $K_3Gd_{1-x-y}(PO_4)_2$:xCe^{3+}, yTb^{3+} phosphors are synthesized by the solid-sate reaction method. X-ray diffraction and photoluminescence spectra are utilized to characterize the structures and luminescence properties of the as-synthesized phosphors. Co-doping of Ce^{3+} enhances the emission intensity of Tb^{3+} greatly through an efficient energy transfer process from Ce^{3+} to Tb^{3+}. The energy transfer is confirmed by photoluminescence spectra and decay time curves analysis. The efficiency and mechanism of energy transfer are investigated carefully. Moreover, due to the non-concentration quenching property of $K_3Tb(PO_4)_2$, the photoluminescence spectra of $K_3Tb_{1-x}(PO4)_2$:xCe^{3+} are studied and the results show that when $x = 0.11$ the strongest Tb^{3+} green emission can be realized.

Keywords: $K_3Gd(PO_4)_2$:Ce^{3+}, Tb^{3+}, energy transfer, photoluminescence

PACS: 85.60.Jb, 78.55.Bq, 75.55.Hx **DOI:** 10.1088/1674-1056/23/2/028505

1. Introduction

White light-emitting diodes (w-LEDs) are considered to be the next illumination source owing to their great advantages, including longer lifetimes, higher rendering indices, higher luminosities, and lower energy consumptions.[1,2] Most commercial w-LEDs have been based on a combination of a blue LED chip and a yellow phosphor: $Y_3Al_5O_{12}$:Ce^{3+} (YAG:Ce).[3] However, a low color-rendering index and high color correlated temperature, because of the lack of red light, seriously affects the quality of w-LEDs.[4] Accordingly, an alternative method of combining ultraviolet (UV) or NUV chips with red, green, blue phosphors has been proposed and attracted a lot of attention.[5] This technology has higher color rendering indexes (CRI) and a higher tolerance to the color variation of a UV chip.[6] Therefore, the exploration of novel tricolor phosphors plays an important role in the progress of w-LEDs.

As is well known, the Tb^{3+} ion is frequently regarded as an activator for green-emitting phosphor due to its dominant $^5D_4-{}^7F_5$ transition peak at around 542 nm.[7,8] However, the intensities of Tb^{3+} absorption peaks are very weak in the 300 nm–400 nm UV region because of strictly forbidden 4f–4f transitions by parity selection rule,[9] which leads to weak green emission of Tb^{3+} ion and this results in the fact that it does not match well with a UV chip. To our best knowledge, Ce^{3+} ions are known to act as highly efficient sensitizers for activators, especially for Tb^{3+} because Ce^{3+} exhibits strong 4f5d absorption in the UV region. Then, the energy transfer from Ce^{3+} to the activator can enhance the light yield of activator under UV light excitation.[4,10] Therefore, one of the strategies to enhance the emission intensity of Tb^{3+} is to co-dope Ce^{3+} ions by utilizing their efficient energy transfer. In addition, an inorganic phosphate with general formula $K_3R(PO_4)_2$ has been put forward because the $K_3R(PO_4)_2$ (R = Nd, Eu, and Tb) show no concentration quenching of luminescence, even though the number of doped activators is large.[11] A reddish orange-emitting phosphor $K_3Eu(PO_4)_2$ was studied by Ju *et al.*,[12] which indicated that the concentration quenching did not take place in this system, even when the doping concentration of Eu^{3+} reached 100%. A similar phenomenon was observed by Mikhailik[13] who studied the luminescence properties of $K_3Tb(PO_4)_2$:Eu excited under VUV. Therefore, there is a possibility that $K_3Gd(PO_4)_2$:Tb^{3+} can serve as an efficient green phosphor in which Tb^{3+} ions contribute to green luminescence. In addition, the emission intensity of green phosphor could be further improved by Ce^{3+} co-doping through energy transfer. Hence, in the present paper, the luminescence properties of $K_3Gd(PO_4)_2$:Tb^{3+} (KGP:Tb^{3+}), $K_3Gd(PO_4)_2$:Ce^{3+}, Tb^{3+}(KGP:Ce^{3+}, Tb^{3+}), $K_3Tb(PO_4)_2$:Ce^{3+} (KTP:Ce^{3+}) phosphors are discussed and the energy transfer process from Ce^{3+} to Tb^{3+} in $K_3Gd(PO_4)_2$ is investigated in detail.

*Project supported by the National Natural Science Foundation of China (Grant Nos. 11204113, 61265004, and 51272097), the Foundation of Application Research of Yunnan Province, China (Grant No. 2011FB022), the Chinese Specialized Research Fund for the Doctoral Program of Higher Education (Grant No. 20115314120001), the Postdoctoral Science Foundation of China (Grant No. 2011M501424), and the National Basic Research Program of China (Grant No. 2011CB211708).

†Corresponding author. E-mail: qiu@kmust.edu.cn

© 2014 Chinese Physical Society and IOP Publishing Ltd

2. Experiment

The phosphors $K_3Gd(PO_4)_2$:Tb^{3+}, $K_3Gd(PO_4)_2$:Ce^{3+}, Tb^{3+}, $K_3Tb(PO_4)_2$:Ce^{3+} were synthesized by the conventional solid-state method. High-purity K_2CO_3 (A.R), Gd_2O_3 (A.R), $NH_4H_2PO_4$ (A.R), TbF_3 (99.99%), CeO_2 (99.99%) were employed as raw materials, which were weighed out and mixed homogeneously by an agate mortar for 30 minutes and placed in an alumina crucible. This crucible had been heated at 950 °C for 6 h under a reducing atmosphere ($5\%N_2 + 95\%H_2$) and slowly cooled to room temperature.

The phases of the obtained samples were identified by X-ray powder diffraction (XRD) with Cu Kα ($\lambda = 1.5418$ Å) radiation in scanning steps of 0.02° in a 2θ range from 10° to 60°, operated at 36 kV and 30 mA (Rigaku Model D/max-2200). The photoluminescence (PL) and photoluminescence excitation (PLE) spectra were measured with a HITACHI F-7000 fluorescence spectrophotometer, using a static 150-W Xe lamp as an excitation source. The fluorescence decay curves were measured by Jobin Yvon FL3 fluorescence spectrophotometer. All the measurements were carried out at room temperature.

3. Results and discussion

The XRD patterns for the $K_3Gd_{1-x-y}(PO_4)_2$:xCe^{3+}, yTb^{3+} phosphors samples with varying Ce^{3+} and Tb^{3+} concentrations are shown in Fig. 1. All of the diffraction peaks are in accordance with those of $K_3Gd(PO_4)_2$ (JCPDS card no. 491085), indicating that the dopant ions have not caused significant changes in the crystal structure of the $K_3Gd(PO_4)_2$ host. The crystal structure of $K_3Gd(PO_4)_2$ belongs to the monoclinic crystal system with space group $P2_1/m$ ($Z = 2$). The basic structural units are composed of isolated GdO_7 decahedron and PO_4 tetrahedron. Each GdO_7 decahedron is connected with six PO_4 tetrahedrons to form two-dimensional $Gd(PO_4)2^{3-}$ sheets in the a–b plane. The K atoms are inserted along the c axis between these sheets.[14] According to the effective ionic radii of cations with different coordination numbers reported by Shannon,[15] we have supposed that Tb^{3+} and Ce^{3+} are preferably expected to occupy Gd^{3+} sites because the ionic radii of Tb^{3+} ($R_{CN=7} = 0.98$ Å) and Ce^{3+} ($R_{CN=7} = 1.07$ Å) are similar to that of Gd^{3+} ($R_{CN=7} = 1.00$ Å). In a $K_3Gd(PO_4)_2$ crystal lattice, there are three different K^+ sites, whose coordination numbers are 9, 10, 11 and their radii are 1.55 Å, 1.59 Å, 1.64 Å respectively. Evidently, they are too big for Tb^{3+} and Ce^{3+} to be occupied. Thus, with the consideration of ionic matching, those Tb^{3+} and Ce^{3+} should occupy Gd^{3+} sites.

Figure 2(a) shows the PLE ($\lambda_{em} = 542$ nm) and PL ($\lambda_{ex} = 373$ nm) spectra of KGP:$0.2Tb^{3+}$ phosphor. The excitation spectrum consists of two broad bands and several sharp lines. The two broad bands centered at 227 nm and 255 nm correspond to the spin-allow transition from the 4f to the 5d state of Tb^{3+} ion, whereas the sharp lines in the range of 320 nm–400 nm are ascribed to excitation due to the forbidden f–f transition of Tb^{3+} ion.[16] The lines located at about 273 nm, 311 nm are supposed to be the excitations of $K_3Gd(PO_4)_2$ host. The PL spectrum shows the characteristic sharp emission lines centered at 485, 542, 580, and 619 nm corresponding to transitions from $^5D_4$ level to the $^7F_6$, $^7F_5$, $^7F_4$, and $^7F_3$ levels of Tb^{3+}.[17] However, emissions in the blue region, which come from the high energy of the $^5D_3$ level, cannot be observed. As the $^5D_3$–$^5D_4$ transition is resonant with the $^7F_6$–$^7F_0$ transition, the emissions of $^5D_3$–^7F_J transitions are often quenched for high Tb^{3+} concentration-doped samples due to the cross relaxation $^5D_3 + {}^7F_6 \rightarrow {}^5D_4 + {}^7F_0$.[18]

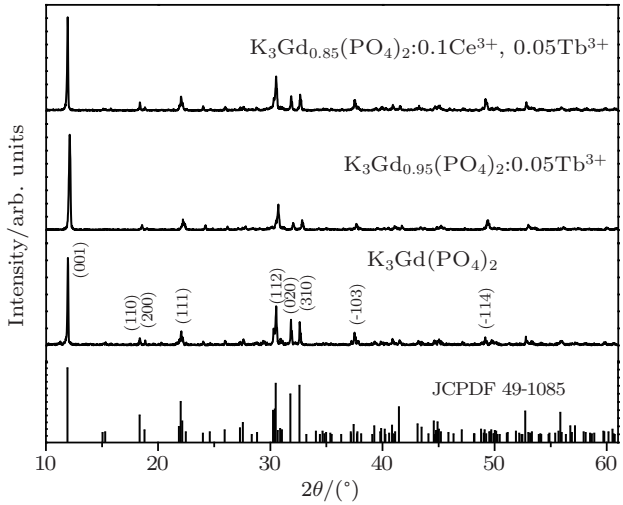


Fig. 1. The XRD patterns of $K_3Gd(PO_4)_2$ $K_3Gd(PO_4)_2$:Tb^{3+}, $K_3Gd(PO_4)_2$:Ce^{3+}, Tb^{3+}.

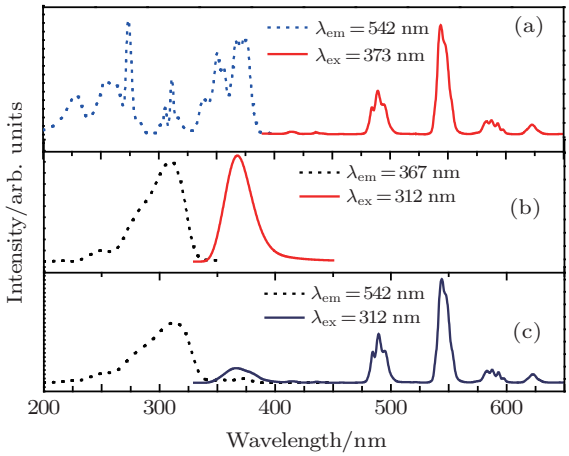


Fig. 2. (color online) PLE and PL spectra of $K_3Gd(PO_4)_2$:$0.2Tb^{3+}$ (a), $K_3Gd(PO_4)_2$:$0.1Ce^{3+}$ (b), $K_3Gd(PO_4)_2$:$0.1Ce^{3+}$, $0.2Tb^{3+}$ (c).

The PLE and PL spectra of KGP:$0.1Ce^{3+}$ are presented in Fig. 2(b). The PLE spectrum of Ce^{3+} single-doped sample exhibits a broad band centered at 312 nm due to the 4f–5d transitions of Ce^{3+} ions. The PL spectrum displays an asymmetrical

broad band centered at 367 nm, which is associated with the transition from the excited state to the $^2F_{5/2}$ and $^2F_{7/2}$ levels of the $4f^1$ ground state configuration.[19,20] From the comparison with the excitation spectrum of Tb^{3+} single-doped sample in Fig. 2(a), it follows that there is an evident overlap between the emission spectrum of KGP:0.1Ce^{3+} and excitation spectrum of KGP:0.2Tb^{3+}, which supports the occurrence of energy transfer from Ce^{3+} to Tb^{3+}. Figure 2(c) shows the PLE and PL spectra of KGP:0.1Ce^{3+}, 0.2Tb^{3+}. The PLE spectrum monitored at 542 nm consists of a broad excitation band, which is similar to that produced by Ce^{3+} ions and the very weak absorptions of Tb^{3+}. The observation of the Ce^{3+} f–d transition in the excitation of Tb^{3+} shows that the Tb^{3+} can be excited through Ce^{3+}, which indicates the possibility of energy transfer from Ce^{3+} to Tb^{3+}. The PL spectrum includes a broadband emission from Ce^{3+} and a group of characteristic emissions of Tb^{3+}, which are centered at 490, 542, 589, and 623 nm corresponding to transitions from the $^5D_4$ level to the $^7F_6$, $^7F_5$, $^7F_4$, and $^7F_3$ levels, respectively.

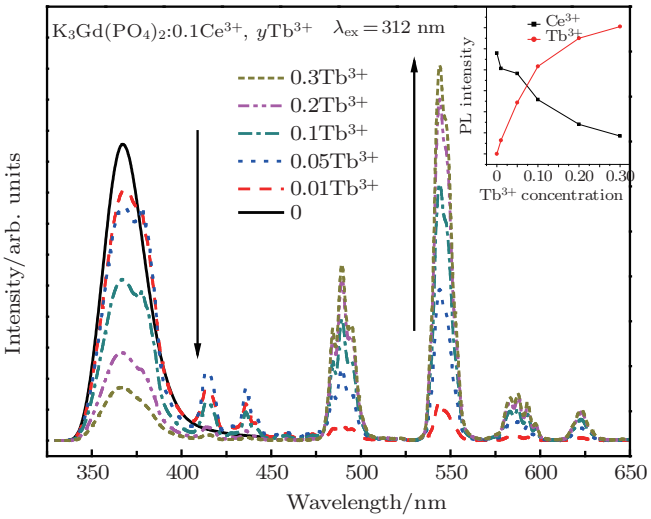


Fig. 3. (color online) PL spectra of $K_3Gd(PO_4)_2$:0.1Ce^{3+}, yTb^{3+} (The inset shows the dependences of PL intensity of Tb^{3+} and Ce^{3+} on Tb^{3+} content in $K_3Gd(PO_4)_2$: 0.1Ce^{3+}, yTb^{3+} phosphor).

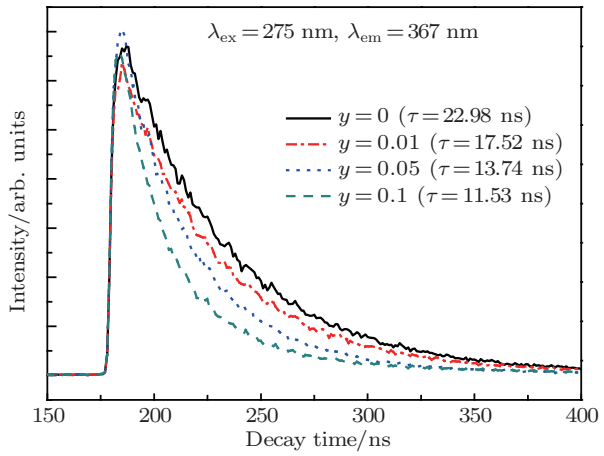


Fig. 4. (color online) Photoluminescence decay curves of Ce^{3+} in $K_3Gd(PO_4)_2$:0.1Ce^{3+}, yTb^{3+} phosphor (excited at 275 nm, monitored at 367 nm).

Figure 3 shows the PL spectra of KGP:0.1Ce^{3+}, yTb^{3+} with varying the Tb^{3+} concentration. Under 312 nm as a characteristic excitation wavelength of Ce^{3+}, the emission peaks of Ce^{3+} as well as sharp emission peaks of Tb^{3+} are observed in the emission spectra of KGP:0.1Ce^{3+}, yTb^{3+}. With the increasing of Tb^{3+} concentration, the emission intensity of Ce^{3+} ion decreases monotonically, whereas that of Tb^{3+} increases simultaneously, which supports the existence of energy transfer from Ce^{3+} to Tb^{3+}. For clarity, the dependences of PL intensity of Tb^{3+} and Ce^{3+} on the content of Tb^{3+} in KGP:0.1Ce^{3+}, yTb^{3+} phosphor are shown in the inset. The PL intensity of Ce^{3+} declines rapidly with the increase of the concentration of Tb^{3+}, whereas the Tb^{3+} characteristic emission intensity strengthens significantly.

In order to further demonstrate the energy transfer from Ce^{3+} to Tb^{3+}, the decay curves of Ce^{3+} emission of KCP:0.1Ce^{3+}, yTb^{3+} phosphors (y = 0, 0.01, 0.05, 0.1) excited at 275 nm and monitored at 367 nm are shown in Fig. 4. It was found that all decay curves can be well fitted by the second-order exponential decay mode, as shown by the following equation:[21]

$$I = A_1 \exp(-t/\tau_1) + A_2 \exp(-t/\tau_2),$$

where I is the luminescence intensity; A_1 and A_2 are fitting parameters; t is the time, τ_1 and τ_2 are the luminescence lifetimes. Based on these parameters, the average decay time τ of Ce^{3+} can be calculated by the following equation:[22]

$$\tau = \frac{A_1\tau_1^2 + A_2\tau_2^2}{A_1\tau_1 + A_2\tau_2}.$$

The values of average decay time (τ) are determined to be 22.98, 17.52, 137.74, 11.53 ns for KGP:0.1Ce^{3+}, yTb^{3+} with y = 0, 0.01, 0.05, 0.1, respectively. It is apparent to observe that τ becomes smaller with the increasing of Tb^{3+} concentration in Ce^{3+}/Tb^{3+} co-doped phosphor. This proves a direct evidence for the energy transfer from Ce^{3+} to Tb^{3+} in the $K_3Gd(PO_4)_2$ host. The energy transfer efficiency η_T of Ce^{3+} to Tb^{3+} can be expressed as follows:[23,24]

$$\eta_T = 1 - \frac{I_s}{I_{so}},$$

where I_{so} and I_s are the luminescence intensities of the Ce^{3+} in the absence and presence of Tb^{3+}, respectively. The energy transfer efficiencies from Ce^{3+} to Tb^{3+} in KGP:0.1Ce^{3+}, yTb^{3+} (y = 0.01, 0.05, 0.1, 0.2, 0.3) are calculated to be 15%, 20%, 46%, 70%, 82% respectively. With the increasing of Tb^{3+} content, the value of η_T increases gradually. Although the content of Tb^{3+} is only 0.3, the efficiency has already reached 80%, which indicates the energy transfer from Ce^{3+} to Tb^{3+} is very efficient. The energy transfer from a sensitizer to an activator may take place via exchange interaction and

electric multipolar interaction. Exchange interaction needs a large or an indirect overlapping between donor and acceptor orbitals, thereby leading to an easy electronic exchange. In addition, Ce^{3+} and Tb^{3+} ions are both reducing ions, such an exchange would require too high energies. Therefore, an energy transfer via exchange interaction is impossible. Thus, the energy transfer from Ce^{3+} to Tb^{3+} occurs through multipolar interaction.[25] According to Dexter's energy transfer formula of multipolar interaction and Reisfeld's approximation,[26,27] we have

$$\frac{\eta_0}{\eta} \propto C_{\mathrm{Ce+Tb}}^{n/3},$$

where η_0 and η are the luminescence quantum efficiencies of the sensitizer (Ce^{3+}) in the absence and presence of activator (Tb^{3+}), respectively. The value of η_0/η can be approximately replaced by the ratio between the relevant luminescence intensities (I_{so}/I_s). C is the total dopant concentration of Ce^{3+} and Tb^{3+}; $n = 6$, 8, and 10, corresponding to the dipole–dipole, dipole–quadrupole, and quadrupole–quadrupole interacitons. The relations between I_{so}/I_s and $C^{n/3}$ when $n = 6$, 8, 10 are illustrated in Fig. 5. It is apparent that the curve for $n = 6$ approaches to the linear relation, implying that the energy transfer from Ce^{3+} to Tb^{3+} is realized mainly through the dipole–dipole interaction.

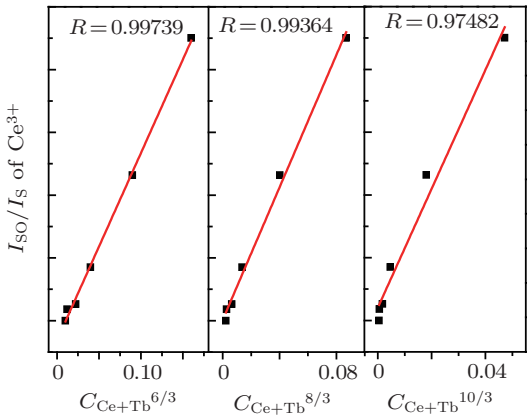


Fig. 5. (color online) Dependences of I_{so}/I_s of Ce^{3+} on $C_{Ce+Tb}^{6/3}$, $C_{Ce+Tb}^{8/3}$, $C_{Ce+Tb}^{10/3}$.

As discussed above, the existence of an energy transfer from Ce^{3+} to Tb^{3+} in KCP was confirmed and their energy transfer efficiency proved to be relatively high. As mentioned above, the $K_3Gd(PO_4)_2$:Tb^{3+} shows no concentration quenching. By utilizing the non-concentration property of $K_3Gd(PO_4)_2$:Tb^{3+} and highly efficient energy transfer between Ce^{3+} and Tb^{3+}, the great green emission can be realized in $K_3Tb(PO_4)_2$:Ce^{3+} phosphor.

Figure 6 exhibits the PL spectra of KGP:xTb^{3+} with different Tb^{3+}-doped concentrations under 373 nm. When $x = 0.05$, the emission peaks at 419, 437, and 459 nm can be observed, which correspond to the transitions $^5D_3$–^7F_J ($J = 5$, 4, and 3) of Tb^{3+} energy level. However, upon increasing Tb^{3+} concentration, the emissions of $^5D_3$–^7F_J can be suppressed due to the cross relaxation effect and transfer of its energy to the $^5D_4$ energy level.[18] From the inset of Fig. 6, it follows that the intensity of Tb^{3+} emission located at 542 nm increases gradually with the increase of Tb^{3+} content and reaches a maximum even when Tb^{3+} entirely occupies the Gd^{3+} sites. This result indicates that the concentration quenching does not take place in this host. To the best of our knowledge, the concentration quenching is caused by energy transfer process among activators, the energy transfer occurs from one activator to another until an energy has sunk in the lattice.[28] Therefore, one possible reason for the non-concentration quenching is that the energy transfer between Tb^{3+}–Tb^{3+} in $K_3Gd(PO_4)$:Tb^{3+} does not occur effectively.

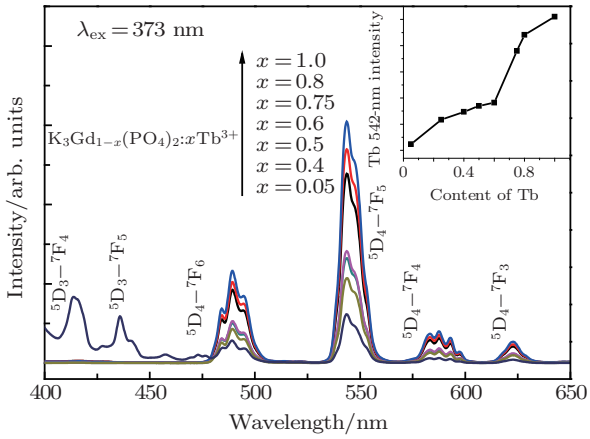


Fig. 6. (color online) PL spectra of $K_3Gd(PO_4)_2$:xTb^{3+} excited by 373 nm (The inset shows the dependences of PL intensity of Tb^{3+} on the content of Tb^{3+} in $K_3Gd(PO_4)_2$:xTb^{3+} phosphor).

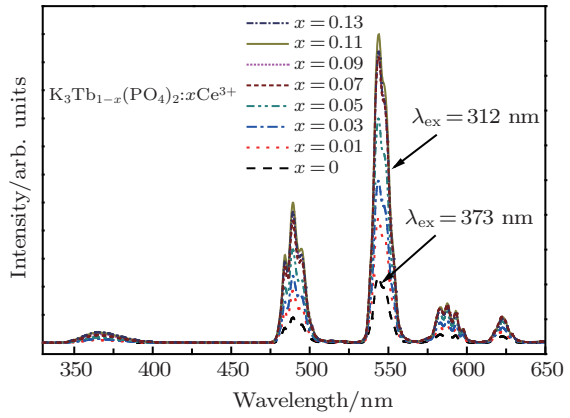


Fig. 7. (color online) PL spectra of of $K_3Tb(PO_4)_2$ under 373 nm and $K_3Tb(PO_4)_2$:xCe^{3+} under 312 nm.

The PL spectra of $K_3Tb(PO_4)_2$ excited by 373 nm and those of $K_3Tb_{1-x}(PO_4)_2$:xCe^{3+} under 312 nm are presented in Fig. 7. The spectra show a weak band emission of Ce^{3+} and intense sharp lines of Tb^{3+}. As can be seen, the intensity of $K_3Tb(PO_4)_2$ under 373 nm is weaker than that of the $K_3Tb(PO_4)_2$:xCe^{3+} phosphor under 312 nm, which is due to

the energy transfer from Ce^{3+} to Tb^{3+}. With the increasing Ce^{3+} concentration, the emission intensities of Ce^{3+} increase continuously and the emission intensities of Tb^{3+} first increase and reach their maximum values at $x = 0.11$ and then decrease. Herein, Ce^{3+} ions replace the lattices of Tb^{3+}, when the Ce^{3+} concentration increases, the Tb^{3+} concentration decreases simultaneously. When the Ce^{3+} concentration varies from 0 to 0.11, the Tb^{3+} green emission is enhanced because the energy transfer is dominant over the decrease of Tb^{3+} concentration. However, when the Ce^{3+} concentration is beyond 0.11, the energy transfer cannot offset the loss of Tb^{3+}. This explains why the Tb^{3+} emission begins to decrease, even though the energy transfer still exists. Figure 8 shows the chromaticity coordinates for $K_3Tb(PO_4)_2$:0.11Ce^{3+} phosphor under 312 nm which are calculated through Zolix Color Convert software and the digital photos under 365-nm UV lamp excitation. It is found that the CIE coordinate for $K_3Tb(PO_4)_2$:xCe^{3+} is (0.297, 0.585) located in the green region, and it shows an intense green light, suggesting that $K_3Tb_{0.89}Ce_{0.11}(PO_4)_2$ phosphor has potential application as a UV-convertible green phosphor in w-LEDs.

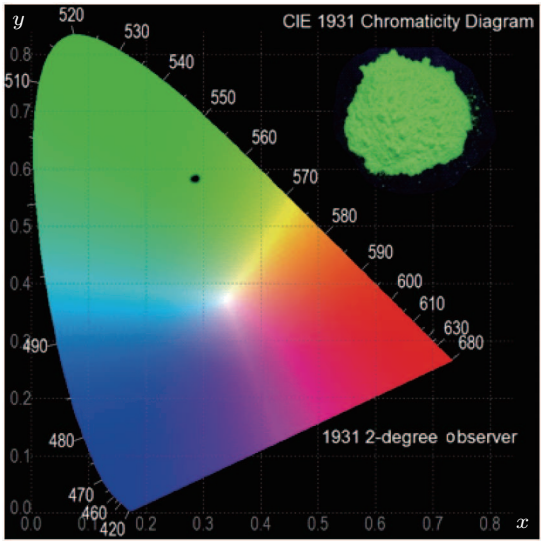


Fig. 8. (color online) Representation of CIE chromaticity coordinates for $K_3Tb(PO_4)_2$:xCe^{3+} phosphors upon 312-nm excitation and the digital photos of $K_3Tb_{0.89}Ce_{0.11}(PO_4)_2$ under 365-nm UV lamp excitation.

4. Conclusions

We successfully synthesized $K_3Gd_{1-x-y}(PO_4)_2$:xCe^{3+}, yTb^{3+} phosphors by the solid-sate reaction method. Co-doping of Ce^{3+} enhances the emission intensity of Tb^{3+} greatly through an efficient energy transfer process from Ce^{3+} to Tb^{3+}. The energy transfer mechanism is demonstrated to be dipole–dipole interaction and its efficiency reaches above 80%. By utilizing the non-concentration quenching of $K_3Tb(PO_4)_2$ and efficient energy transfer from Ce^{3+} to Tb^{3+}, the $K_3Tb(PO_4)_2$:Ce^{3+} phosphors are prepared and exhibit a strong green emission, which indicates that $K_3Tb(PO_4)_2$:Ce^{3+} phosphors have potential applications in serving as a UV-convertible phosphor for emitting green light.

References

[1] Zhou T L, Song Z, Song X P, Bian L and Liu Q L 2010 *Chin. Phys. B* **19** 127808
[2] Wei X D, Cai L Y, Lu F C, Chen X L, Chen X Y and Liu Q L 2009 *Chin. Phys. B* **18** 3555
[3] Bachmann V, Ronda C and Meijerink A 2009 *Chem. Mater.* **21** 2077
[4] Li P L, Wang Y S, Zhao S L, Zhang F J and Xu Z 2012 *Chin. Phys. B* **21** 127804
[5] Han J Y, Im W B, Lee G Y and Jeon D Y 2012 *J. Mater. Chem.* **22** 8793
[6] Chen Y, Gong M, Wang G and Su Q 2007 *Appl. Phys. Lett.* **91** 071117
[7] Jiao H and Wang Y 2009 *J. Electrochem. Soc.* **156** J117
[8] Nigam S, Sudarsan V, Vatsa R K, Ghattak J and Satyam P 2009 *J. Phys. Chem. C* **113** 8750
[9] Yu H, Zi W, Lan S, Gan S, Zou H, Xu X and Hong G 2012 *Opt. Laser Technol.* **44** 2306
[10] Han B, Zhang J and Lü Y 2013 *J. Am. Ceram. Soc.* **96** 179
[11] Hong H P and Chinn S 1976 *Mater. Res. Bull.* **11** 421
[12] Ju G, Hu Y, Chen L, Wang X, Mu Z, Wu H and Kang F 2012 *Opt. Laser Technol.* **44** 39
[13] Mikhailik V, Kraus H and Dorenbos P 2009 *Res. Lett.* **3** 13
[14] Zhao D and Li F F 2010 *Acta Crystallographica Section E: Struct. Rep. Online* **66** i64
[15] Shannon R 1976 *Acta Crystallogr Sect. A* **32** 751
[16] Kuo T W and Chen T M 2010 *J. Electrochem. Soc.* **157** J216
[17] Pavitra E, Raju G S R, Ko Y H and Yu J S 2012 *Phys. Chem. Chem. Phys.* **14** 11296
[18] Sun J, Lai J, Xia Z, Zhang X, Liu H and Du H 2012 *Appl. Phys. B* **107** 827
[19] Li Y Q, Hirosaki N, Xie R J, Li J, Takeda T, Yamamoto Y and Mitomo M 2009 *J. Am. Ceram. Soc.* **92** 2738
[20] Dorenbos P, Van Loef E, Van Eijk C, Krämer K and Güdel H 2003 *Phys. Rev. B* **68** 125108
[21] Pang R, Li C, Shi L and Su Q 2009 *J. Phys. Chem. Solids* **70** 303
[22] Murakami S, Herren M, Rau D and Morita M 2000 *Inorg. Chim. Acta* **300** 1014
[23] Yang W J and Chen T M 2006 *Appl. Phys. Lett.* **88** 101903
[24] Paulose P, Jose G, Thomas V, Unnikrishnan N and Warrier M 2003 *J. Phys. Chem. Solids* **64** 841
[25] Chiu Y C, Liu W R, Yeh Y T, Jang S M and Chen T M 2009 *J. Electrochem. Soc.* **156** J221
[26] Xia Z G and Liu R S 2012 *J. Phys. Chem. C* **116** 15604
[27] Huang C H and Chen T M 2011 *J. Phys. Chem. C* **115** 2349
[28] Zhang X M and Seo H J 2010 *J. Alloys Compd.* **503** L14